Available online at www.sciencedirect.com
ScienceDirect
Journal of Hazardous Materials 150 (2008) 565–572
Journal of Hazardous Materials
www.elsevier.com/locate/jhazmat

Removal of As(III) in a column reactor packed with iron-coated sand and manganese-coated sand

Yoon-Young Chang, Ki-Hoon Song, Jae-Kyu Yang *

Department of Environmental Engineering, Kwangwoon University, Seoul 139-701, Republic of Korea

Received 10 November 2006; received in revised form 20 February 2007; accepted 4 May 2007
Available online 10 May 2007

Abstract

The applicability of manganese-coated sand (MCS) and iron-coated sand (ICS) for the treatment of As(III) via oxidation and adsorption processes was investigated. Scanning electron microscopy (SEM) and X-ray diffraction spectroscopy (XRD) were used to observe the surface properties of the coated layer. In the batch adsorption, the adsorption rate of As(V) onto ICS was greater than that of As(III), and ICS showed a greater adsorption capacity for the removal of As(V) than As(III). From a bench-scale column test, a column reactor packed with both MCS and ICS was found to be the best system for the treatment of As(III) due to the promising oxidation efficiency of As(III) to As(V) by MCS and adsorption of As(V) by both MCS and ICS. From these bench-scale results, the treatment of synthetic wastewater contaminated with As(III) was investigated using a pilot-scale filtration system packed with equal amounts (each 21.5 kg) of MCS at the bottom and ICS on the top. The height and diameter of the column were 200 and 15 cm, respectively. As(III) solution was introduced into the bottom of the filtration system, at a speed of 5×10^{-3} cm s^{-1}, over 148 days. The breakthrough of total arsenic in the mid-sampling (end of the MCS bed) and final-sampling (end of the ICS bed) positions began after 18 and 44 days, respectively, and showed complete breakthrough after 148 days. Although the breakthrough of total arsenic in the mid-sampling position began after 18 days, the concentration of As(III) in the effluent was below 50 μg L^{-1} for up to 61 days. This result indicates that MCS has sufficient oxidizing capacity for As(III), and 1 kg of MCS can oxidize 93 mg of As(III) for up to 61 days. When the complete breakthrough of total arsenic occurred, the total arsenic removed by 1 kg of MCS was 79.0 mg, suggesting MCS acts as an adsorbent for As(V), as well as an oxidant for As(III). From this work, a filtration system consisting of both MCS and ICS can potentially be used a new treatment system to simultaneously treat As(III) and As(V).

Keywords: Adsorption; Arsenic; Iron-coated sand; Manganese-coated sand; Oxidation

1. Introduction

Arsenic is generally found as a contaminant in soil and water systems due to various anthropogenic sources, such as mining activity, discharges of industrial wastes and agricultural application, as well as from geochemical reactions [1–3]. The elevated concentrations of arsenic in the water system originating from the natural source have been attributed to pyritic sedimentary rocks in contact with the aquifer. As arsenic causes serious environmental problems in water systems, and is known as a primary concern to humans exposed to such systems, the World Health Organization (WHO) has recommended lowering the As-drinking water standard 10 μg L^{-1} [4]. Although arsenic has multiple oxidation states (+5, +3, 0 and −3), arsenite As(III) and arsenate As(V) are the most common in natural environments. Generally, As(III) has been reported as the preferential state in sediment or the aqueous phase under anaerobic conditions, while the As(V) species occurs in the sediment under aerobic conditions [5]. The speciation and solubility of inorganic arsenic is sensitive to both the redox conditions and pH of the environments, which affects the toxicity and mobility of arsenic in soils [6–8]. To treat arsenic in water systems, several methods have been employed, such as adsorption, coagulation, membranes or electrolysis [9]. Twindell et al. [10] reported the precipitation of Fe(III)-arsenate or arsenate co-precipitation with excess iron (Fe/As > 3 mol mol^{-1}). Granular activated alumina has been applied for the removal of As from water [11,12]. However, some of these processes are expensive or require the control of pH

* Corresponding author. Tel.: +82 2 940 5769; fax: +82 2 917 5769.
E-mail address: jkyang@kw.ac.kr (J.-K. Yang).

0304-3894/$ – see front matter © 2007 Elsevier B.V. All rights reserved.
doi:10.1016/j.jhazmat.2007.05.005

and/or other parameters to achieve the optimum arsenic removal capacity; therefore, a more effective and economical technique would be highly desirable. In addition, most of the processes that have been identified as promising techniques in the treatment of As(V) [9] are also partly effective for the treatment of As(III), thus require a further simple and cost-effective technique as a pretreatment for the oxidation of As(III) to As(V). Therefore, as one of the promising techniques, manganese coated sand (MCS) and iron-coated sand (ICS) was applied for the treatment of both As(III) and As(V) [13]. Joomoonjin sand is widely used in Korea as filtration sand; thus, many applications of this sand have been reported for the treatment of wastewater using ICS and/or MCS preparations [13–15]. In previous studies, ICS was shown to have an important capacity for the removals of As(III) and As(V) through adsorption. Also, MCS showed a good oxidation capacity for As(III). However, until now, limited information has been available on the simultaneous treatment of As(III) and As(V) using MCS and ICS by considering a real groundwater situation.

In this study, as a promising technique for the treatment of As(III), MCS and ICS synthesized using Joomoonjin sand was used to treat a synthetic wastewater contaminated with As(III). The effectiveness of the filtration system with both MCS and ICS for removing As(III) from solution through the oxidation of As(III) by MCS, as well as adsorption of As(V) on MCS and ICS, was assessed using both bench-scale and pilot-scale column reactors.

2. Materials and methods

Joomoonjin sand, standard sand found in Korea, with a particle size ranging from 1.0 to 1.2 mm, was used as the supporting material for iron and manganese. Prior to coating iron and manganese onto the sand, the sand was pre-washed with 0.1 M HCl for 2 h and rinsed three times with deionized water to remove any impurities. All chemicals were of analytical grade. $FeCl_3$ and $Mn(NO_3)_2$ was purchased from Aldrich Chemicals. The $NaNO_3$ used to fix ionic strength was obtained from Fisher Scientific. All solutions were prepared with deionized water (18 MΩ cm) prepared using a Hydro-Service reverse osmosis/ion exchange apparatus (Model LPRO-20). All bottles and glassware were acid washed and rinsed with deionized water before use.

2.1. Preparation of iron-coated sand and manganese-coated sand

In order to prepare MCS, a $Mn(NO_3)_2$ solution (0.1 mol L^{-1}), previously adjusted to pH 8 with NaOH solution, was mixed with Joomoonjin sand at 1.2 kg L^{-1} in a purpose built pilot-scale reactor. This reactor was designed so the surface could be heated with liquefied petroleum gas, with each batch having a sand capacity of 200 kg. By rotating the reactor at 30 rpm, the water in the suspension was continuously removed by heating at 150 ± 5 °C until approximately only 10% of the water remained in the suspension. The reactor was then rotated at a reduced speed (15–20 rpm) for 1-h to allow stabilization of the coating process. To remove traces of uncoated manganese on the sand, the dried sand was rinsed several times with distilled water and then dried at 105 °C. In the preparation of ICS, a $FeCl_3$ solution (0.1 mol L^{-1}), previously adjusted to pH 12 with NaOH solution, was mixed with Joomoonjin sand at 1.2 kg L^{-1} in the pilot-scale reactor. The same procedure used in the preparation of MCS was then followed. The manganese and iron coated onto the sand were stripped using an acid digestion method (U.S.EPA 3050B). After filtration, the dissolved manganese and iron concentrations were measured using an inductively coupled plasma (ICP-AES, model Optima 2000 DV, Perkin Elmer Co.). The mineralogy of the ICS and MCS was characterized by X-ray diffraction (XRD, model D/MAX, Rigaku). Photomicrography of the exterior surface of the Joomoonjin sand, both ICS and MCS, was obtained by Scanning Electron Microscopy (SEM, model JSM-5900, JEOL).

2.2. Experimental methods

The adsorption kinetics of As(III) and As(V) onto ICS or raw Joomoonjin sand were obtained at an initial pH of 6.5, with a constant ionic strength (0.01 mol L^{-1} $NaNO_3$) at various times. The initial arsenic concentration and soil to solution ratio (S/S) were 1 mg L^{-1} and 5 g L^{-1}, respectively. A pH-edge adsorption experiment was performed for 24 h at room temperature (23–25 °C) with variation of pH from 2 to 10, with an S/S ratio of 5 g L^{-1}. In order to find the best column configuration for the removal of As(III), column systems having different ICS and MCS compositions in the bench-scale column reactor were applied at room temperature (23–25 °C). One of the objectives of this research was to identify the applicability of a filtration system employing both ICS and MCS for the treatment of groundwater contaminated with arsenic at around neutral pH; therefore, all experiments were perform at pH 6.5. Ten grams each of the ICS and/or MCS were packed into a column; two-staged; equal amounts of ICS and MCS, or MCS-alone. The pore volume (V_o) in the column packed with both ICS and MCS was 4.4 cm^3 when the porosity (Φ) was assumed to be 0.33, with a total column depth of 17 cm. For the column experiments, the arsenite solution (1 mg L^{-1}), with a constant ionic strength at 0.01 M $NaNO_3$, was pumped upward through the bottom of the column, using an Acuflow Series II high-pressure liquid chromatography pump, at a flow rate of 0.4 mL min^{-1}. Effluent samples were then obtained using Spectra/Chrom CF-1 Fraction Collectors. After filtration of the samples with 0.45 μm syringe filters, a portion of the sample was subjected to a modified anion exchange method [16] to quantify the As(III) and As(V). The chloride form of the anion-exchange resin (Dowex $1 \times 8 - 100$, sigma) was converted to the acetate form in a glass-column ($d = 0.8$ cm, 1.5 mL resin). Prior to the separation of As(III) and As(V), the pH of each sample was adjusted to around 3.5. Under this condition, the fully protonated As(III) passes through the column, while the partly deprotonated As(V) was retained. Prior to sample analysis, the column performance was tested with both As(V) and As(III) dissolved in aqueous solution. The As(III) recovery was >87%, while complete retention of As(V) was observed. The total dissolved arsenic concentration before the column test and As(III) concentration in the column

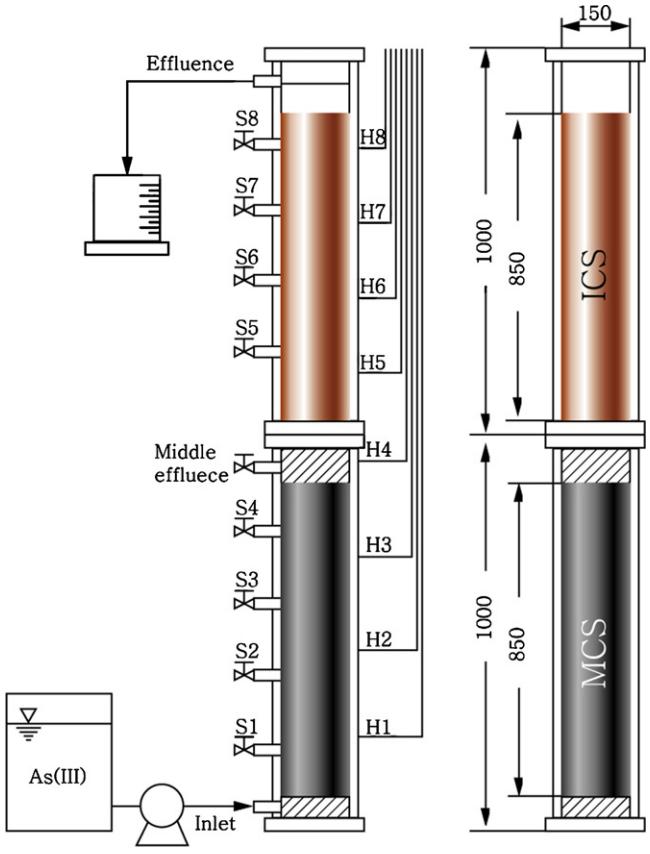

Fig. 1. Schematic apparatus of reactive sand filtration tower (RSFT) (scale unit: mm) (21.5 kg MCS, 21.5 kg ICS, initial As(III) = 1.0 mg L^{-1}, v = 0.005 cm s^{-1}, Q = 22.5 mL min^{-1}).

effluent were measured using an ICP. The As(V) concentration was then calculated by difference.

A pilot-scale As(III) removal experiment was conducted in a column reactor at room temperature (23–25 °C), with a constant initial pH of 6.5. Fig. 1 shows a schematic diagram of the apparatus of the pilot-scale column reactor. The detailed specifications of the column reactor and composition of the artificial ground water pollutant are shown in Tables 1 and 2, respectively. In the column, 21.5 kg of each ICS and MCS were packed as a two-staged column. The arsenite solution (1 mg L^{-1}), with a constant ionic strength at 0.01 mol L^{-1} $NaNO_3$, was pumped upward through the bottom of the column at a linear velocity of 5×10^{-3} cm s^{-1}. Effluent samples were then collected every day at constant time intervals. After filtration of the samples with 0.45 μm syringe filters, a portion of the sample was subjected to a modified anion exchange method [16] to quantify the As(III) and As(V). The concentrations of dissolved total As and As(III) were measured using an ICP. To record the headloss with operating time, pipes were installed at a constant height within the column.

Table 1
Specification of RSFT and operating parameters

Specification of RSFT	Operating parameters
Material of reactor	Acryl
Reactor height (H_T)	200 cm
Reactor diameter (D_T)	15 cm
Reactor volume (V_T)	35,325 cm^3
Reactor pore volume (PV_T)	15,244 cm^3
Flow rate (Q)	22.5 ml min^{-1}
Linear velocity (v)	5×10^{-3} cm s^{-1}
MCS bed height (H_{MCS})	85 cm
MCS bed volume (V_{MCS})	15,013 cm^3
MCS bed pore volume (PV_{MCS})	6,230 cm^3
Retention time of MCS bed (θ_{MCS})	4.72 h
ICS bed height (H_{ICS})	85 cm
ICS bed volume (V_{ICS})	15,013 cm^3
ICS bed pore volume (PV_{ICS})	6,365 cm^3
Retention time of ICS bed (θ_{ICS})	4.72 h

3. Results and discussion

3.1. Preparation of ICS and MCS

Using previously reported ICS and MCS preparation methods under optimum conditions on a bench scale, the ICS and MCS in the pilot plant were prepared with Joomoonjin sand as a supporting material, with particle sizes ranging from 1.0 to 1.2 mm [13]. The original iron content in the raw sand was 2500 mg kg^{-1}. From the coating process, 3150 mg kg^{-1} iron and 3960 mg kg^{-1} manganese were loaded onto raw Joomoonjin sand. The amounts of iron and manganese coated onto the sand were obtained by subtracting the control amount from the total iron and manganese measured using an acid digestion method (U.S.EPA 3050B). After filtration, the resultant acidic solution was diluted and the iron and manganese contents then measured using an ICP. Fig. 2a and b shows the X-ray diffraction spectra obtained for ICS and MCS using Cu Kα radiation (λ = 1.5406 Å) at kV = 40 and mA = 100, with a Scan Speed = 2.4θ min^{-1} and Scan Range = 10–80θ. Comparing the XRD peak information of Fig. 2a with the JCPDS file, the peaks were identified as the mixture of hematite and goethite. Also comparing the XRD peak information of Fig. 2b with the JCPDS file, the peaks were well matched to those of pyrrolusite (δ-MnO_2). The mineralogy of the iron coated onto the surface of the ICS is known to depend on the coating temperature [17]. From the coating of Fe(III) on silica, Lo et al. [17] found amorphous iron oxides coating at 60 °C, goethite and hematite at 150 °C and hematite at above 300 °C. Scanning electron microscopy was used to identify the mor-

Table 2
Composition of the artificial ground water pollutant

Ingredient	As(III)	Ca^{2+}	CO_3^{2-}	Na^+	Cl^-	K^+	NO_3^-	Mg^{2+}	SO_4^{2-}	pH
Concentration (mg L^{-1})	1.0	20	30	4.6	7.1	1.6	2.5	1.5	7.7	6.5
Concentration (mM)	0.01	0.5	0.5	0.2	0.2	0.04	0.04	0.06	0.08	

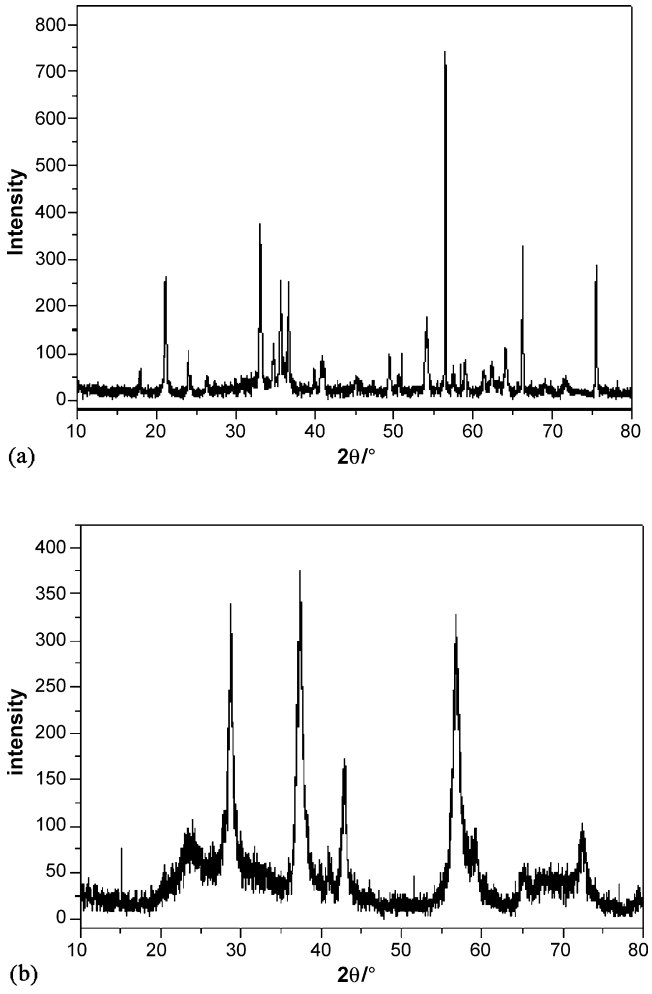

Fig. 2. X-ray diffraction spectrum of (a) ICS and (b) MCS.

phology of the coated metallic species. The SEM photographs shown in Fig. 3a–c were taken at 10,000× magnification to observe the surface morphologies of natural Joomoonjin sand, ICS and MCS, respectively. The SEM images of acid-washed natural Joomoonjin sand in Fig. 3a show very ordered silica crystals at the surface. The natural Joomoonjin sand had a relatively uniform and smooth surface, with small cracks, micropores or light roughness found on the sand surface. The ICS (Fig. 3b) had significantly rougher surfaces than the Joomoonjin sand.

3.2. Batch adsorption

Fig. 4 shows the adsorption trends for As(III) and As(V) onto the ICS, and of As(V) onto uncoated sand as a control, over time. The adsorption of As(V) onto the ICS was completed within 20 min, while that of As(III) was relatively slower, and did not reach equilibrium after 300 min. The uncoated sand also showed rapid removal of As(V), reaching adsorption equilibrium within 20 min. Due to the presence of 0.24% (w/w) iron in the uncoated sand, the Joomoonjin sand has a particular adsorption capacity itself, and removed 24% of the initial As(V) concentration. However, the removal capacity was rather less than that of ICS,

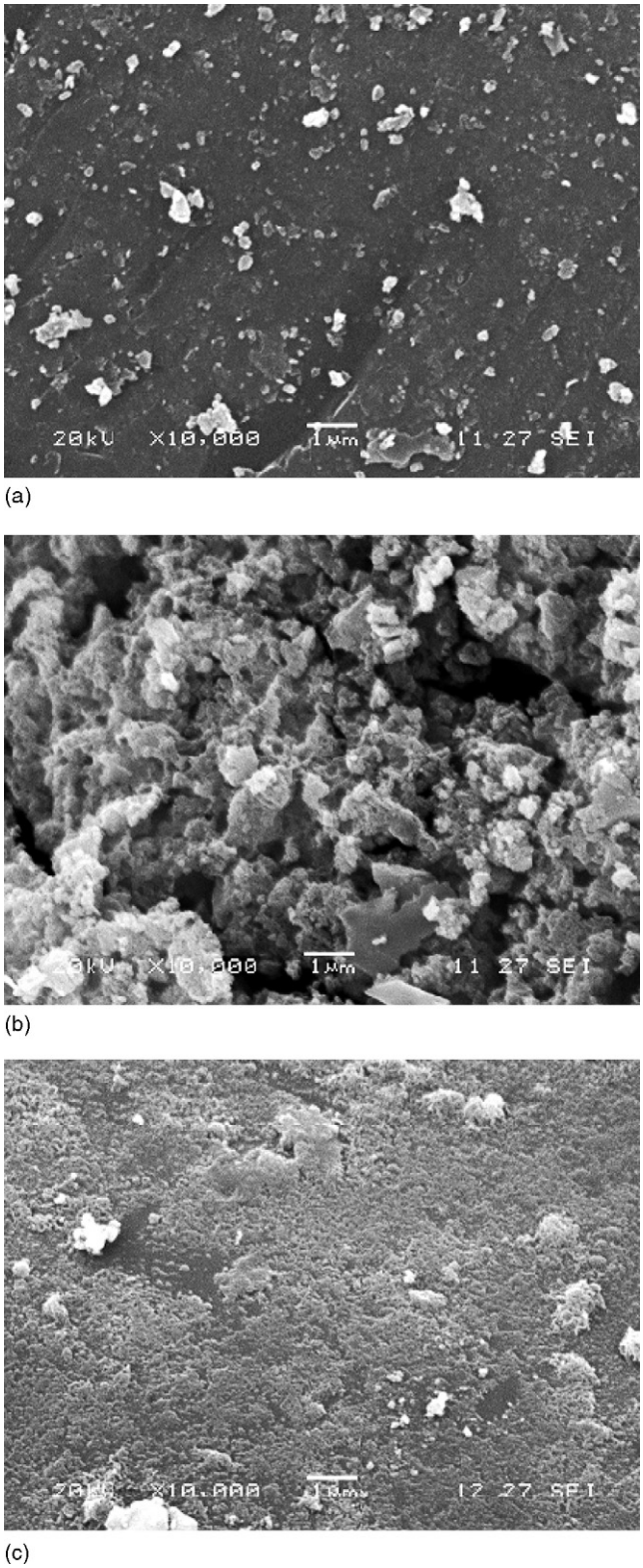

Fig. 3. SEM image for (a) Joomoonjin sand, (b) ICS and (C) MCS.

suggesting comparative limitation for the use of Joomoonjin sand itself in the removal of arsenic.

From the batch adsorption with variation in pH, the As(V) was found to follow an anionic-type of adsorption, resulting complete removal below pH 7 and even 90% removal at pH

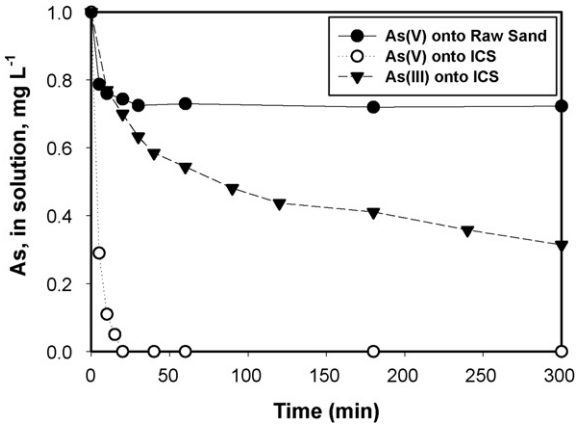

Fig. 4. Adsorption kinetics arsenic onto ICS and raw sand (initial As = 1.0 mg L^{-1}, S/S = 5 g L^{-1}, ionic strength = 0.01 M $NaNO_3$).

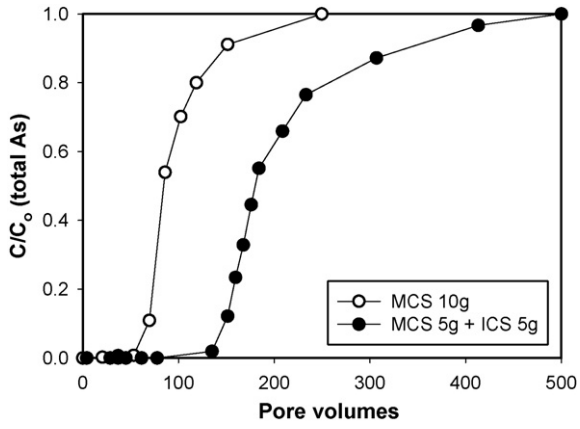

Fig. 6. Total As concentration in the effluent of two column systems (initial As = 1.0 mg L^{-1}, ionic strength = 0.01 M $NaNO_3$, initial pH = 6.5).

10, as shown in Fig. 5. This result suggests a strong surface complex between the Fe(III) (mixture of hematite and goethite) on the surface of the ICS and As(V).

From spectroscopic analyses, Goldberg and Johnston reported that arsenate and arsenite form inner-sphere complexes on amorphous Fe oxide [18]. Iron(hydr-)oxides, such as ferrihydrite and goethite, are known to form inner-sphere complexes with arsenate via the formation of monodentate and bidentate complexes [19–21]. Conversely, the As(III) adsorption onto the ICS was below 50% over the entire pH range studied, but showed slightly favorable adsorption at near neutral pH. From our previous studies [14] regarding the adsorption isotherm of arsenic onto ICS and MCS at pH 4.5, with variation in the initial arsenic concentration, the adsorption isotherm was well described by the Langmuir-type ($q = QC_e b/(1 + C_e b)$). The maximum adsorptions of As(III) and As(V) onto the ICS (Q, denoted as mg kg^{-1}) were found to be 94 and 165 mg kg^{-1}, respectively. The Q value of As(V) was over two-times greater than that of As(III). The maximum adsorption of As(V) onto the MCS was also reported to be 60 mg kg^{-1}, which was approximately three-times lower than that onto the ICS.

3.3. Bench-scale column experiments

Fig. 6 shows the breakthrough curves of arsenic from two different column systems. In the MCS-alone system, the arsenic breakthrough occurred after 50 pore volumes and reached near complete breakthrough after 250 pore volumes. After the breakthrough of arsenic, the concentration of As(III) in the effluents was below 20 μg L^{-1} over the entire reaction period, with most of the arsenic identified as As(V) due to the near complete conversion of As(III) to As(V) by the MCS. This result suggests that the catalytic activity of MCS on the oxidation of As(III) is valid for much longer after the initial breakthrough of arsenic. Compared to the MCS-alone system, the breakthrough of total arsenic in the two-staged column was significantly delayed, and most of the arsenic in the effluent was also identified as As(V) due to the near complete oxidation of As(III) to As(V). Therefore, this result suggests that the two-staged column system has advantages in the oxidation of As(III) and for the removal of As(V) via adsorption by both the ICS and MCS.

3.4. Pilot-scale column experiments

The breakthrough of arsenic was tested using the pilot-scale column system separately packed with equal amounts of ICS

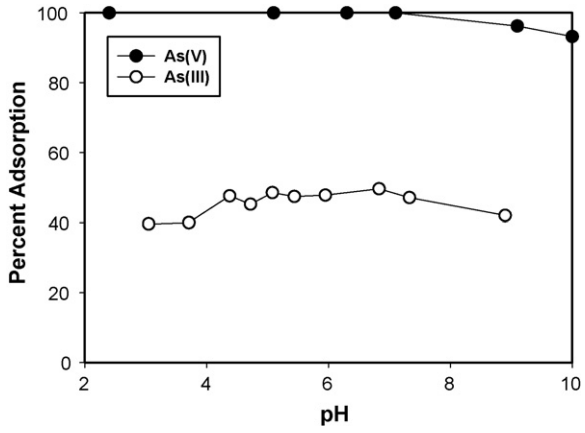

Fig. 5. Adsorption of arsenic onto ICS as a function of pH (S/S = 5 g L^{-1}, ionic strength = 0.01 M $NaNO_3$).

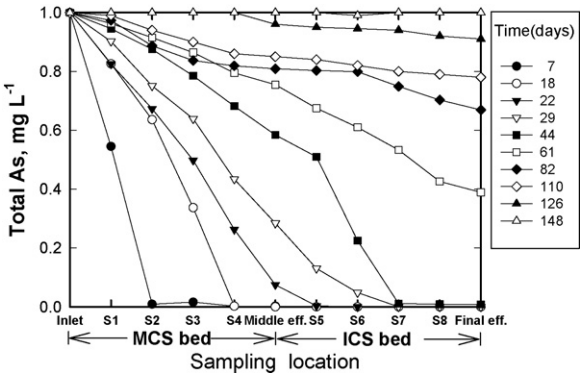

Fig. 7. Concentration of total arsenic at each sampling position with variation of operating time.

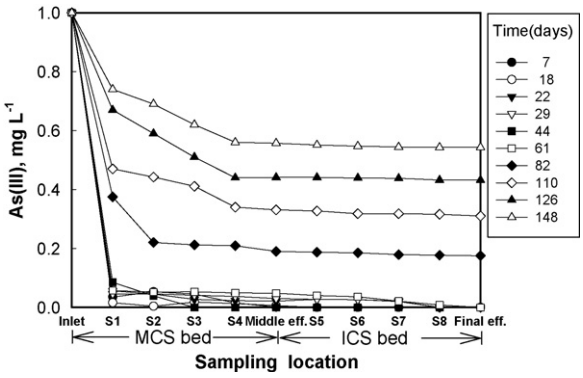

Fig. 8. Concentration of As^{3+} at each sampling position with variation of operating time.

and MCS. Figs. 7–9 show the breakthrough curves of arsenic up to day 148. In order to observe the oxidation trends of As(III) in the MCS bed and removal trends of arsenic in the ICS bed, five samples were simultaneously collected from different heights of both the MCS and ICS beds (s1, s2, s3, s4 and middle effluent, and s5, s6, s7, s8 and final effluent, respectively). The breakthrough of total arsenic from the final effluent occurred after 44 days, as shown in Figs. 7 and 9. Fig. 8 shows the fraction of As^{3+} in the effluent at each sampling point with variation in the operating time. Due to the effective oxidation capacity of MCS for As(III), most of the arsenic in the middle and final effluents were identified as As(V) for up to 61 days; although breakthrough was observed at day 44. The percent oxidation of As(III) measured at the three different sampling positions (S_1, middle and final) are shown in Fig. 10. The percent oxidation was above 90% up to day 61, but thereafter was significantly decreased at all sampling positions. This result matched the fraction of As^{3+} in Fig. 8 quite well. These results suggest that 1 kg of MCS can oxidize 93 mg of As(III) without losing any oxidation power. The type of MnO_2 on the sand may vary, such as α-MnO_2, β-MnO_2 or δ-MnO_2, depending on the preparation conditions. However, Oscarson et al. [22] reported that any type of MnO_2 can effectively remove As(III) via oxidation and adsorption. The redox potentials of Mn(III)/Mn^{2+} and Mn(IV)/Mn^{2+} are +1.50 and

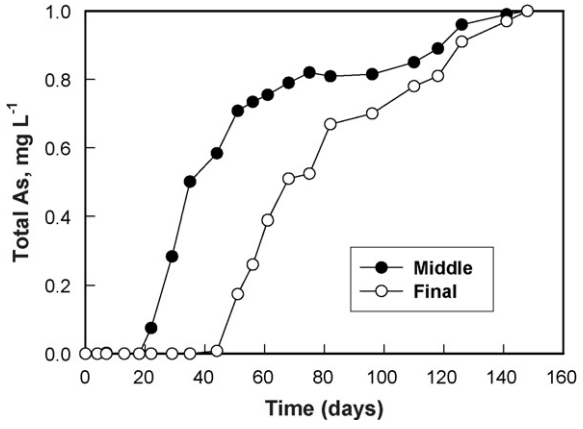

Fig. 9. Breakthrough of total arsenic at middle and final sampling position with variation of operating time.

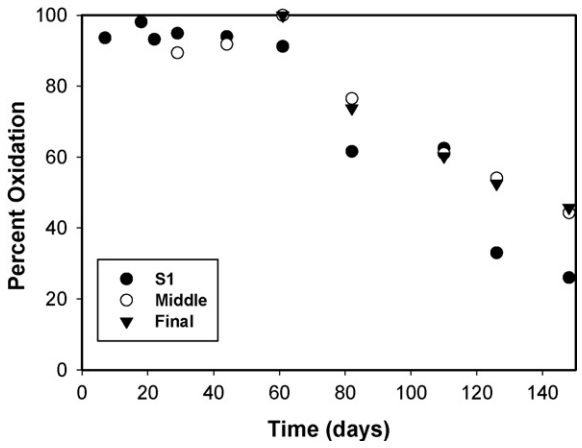

Fig. 10. Percent oxidation of As(III) at three different sampling position with variation of operating time.

+1.23 V, respectively. As the redox potential of As(III)/As(V) is +1.18 V, As(III) can be thermodynamically oxidized to As(V) by both Mn(III) and Mn(IV).

$$\mathrm{Mn(III)OOH(s)} + 3\mathrm{H^+} + \mathrm{e^-} = \mathrm{Mn^{2+}} + 2\mathrm{H_2O}, \quad E^0 = +1.50\,\mathrm{V} \tag{1}$$

$$\mathrm{Mn(IV)O_2(s)} + 4\mathrm{H^+} + 2\mathrm{e^-} = \mathrm{Mn^{2+}} + 2\mathrm{H_2O}, \quad E^0 = +1.23\,\mathrm{V} \tag{2}$$

$$\mathrm{As(III)} \rightarrow \mathrm{As(V)}, \quad E^0 = +1.18\,\mathrm{V} \tag{3}$$

As shown in Fig. 9, the breakthrough of total arsenic started after 18 days, with complete breakthrough occurring after 150 days. The total arsenic absorbed onto the MCS after complete breakthrough was 79.0 mg for 1 kg of the MCS. Therefore, MCS acts as an oxidant for As(III) as well as an adsorbent for As(V). The possibility of the adsorption of As(V) onto the MCS has been verified by our previous result obtained in a batch experiment with variation in pH [15]. The maximum adsorption of As(V) onto the MCS was reported to be 60 mg kg^{-1}, which was somewhat lower than the As(V) removed in the column experiment in this work. The ICS has also been reported to have a greater capacity for the removal of As(V) than As(III), as well as for the removal of As(V) compared to the MCS. Therefore, the As(V) not removed by the MCS bed was removed by the ICS, with a very lower concentration of total arsenic observed in final effluents. Over the entire reaction period, the effluent pH was little changed from that of the initial influent, which was between 6.5 and 7.0.

In order to investigate the stability of the iron and manganese coated onto the ICS and MCS, respectively, during the column test, soluble iron and manganese in samples collected from all of the sampling positions were analyzed. Fig. 11 shows that during the initial reaction the dissolution of Mn^{2+} was rapid, and then reached to a maximum concentration of 2 mg L^{-1}. After 60

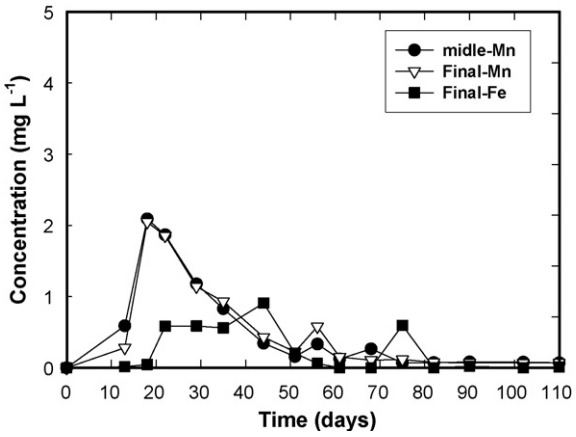

Fig. 11. Variation of the soluble Mn and Fe concentration at middle and final sampling position with variation of operating time.

days, a reasonably constant Mn^{2+} concentration was observed. In the case of iron, the maximum concentration ($\sim$1 mg L^{-1}) was observed at around day 44. During the entire reaction period, the soluble iron released was always below the emission standard for iron (2 mg L^{-1}) into clean water areas within KOREA. However, the soluble Mn^{2+} released during the initial reaction reached that of the emission standard (2 mg L^{-1}). Therefore, if a filtration system packed with both ICS and MCS is applied in the treatment of groundwater or surface water contaminated with As(III), further studies on the stability of MCS or a post-treatment system of Mn^{2+} will be required.

The variation in the head loss of the column system during the process is shown in Fig. 12. Each *h* denotes the height difference in relation to the top of the column system. The head losses in the MCS bed were expressed from *h*1 to *h*4 and those in the ICS bed from *h*5 to *h*8, depending on the height of reactor. No distinct variation in the head loss was observed at all points over the entire reaction period. This result distinctly suggests that the filtration system used in this study can be applied long term, without losing any retention time during the operating process.

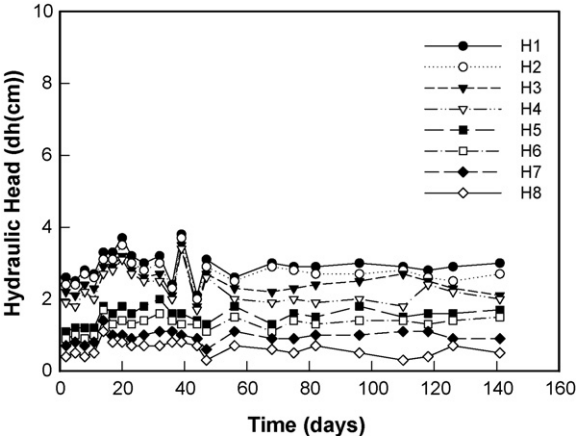

Fig. 12. Variation of head loss at each sampling position.

4. Conclusions

From this research, MCS and ICS were identified as good filter materials for the removal of As(III) through the promising oxidation efficiency of As(III) to As(V) by the MCS and the adsorption of As(V) by both the MCS and ICS. In a pilot-column reactor, the breakthrough of total arsenic in the mid-sampling position began after 18 days; however, the concentration of As(III) in the effluent was below 50 μg L^{-1} up to day 61 due to the sufficient oxidizing capacity of the MCS for As(III). When complete breakthrough of total arsenic occurred, the total arsenic removed by the MCS was 79.0 mg with 1 kg of MCS, suggesting MCS acts as an oxidant for As(III) as well as an adsorbent for As(V). In addition to the efficient removal efficiency of As(III), the filtration system with both MCS and ICS showed no significant head loss over the entire reaction period.

Acknowledgements

The present research was funded by a Research Grant of Kwangwoon University in 2006 and an Unibiz Research Grant of Small and Medium Business Administration.

References

[1] D.K. Bhumbla, R.F. Keefer, Arsenic mobilization and bioavailability in soils, in: J.O. Nriagu (Ed.), Arsenic in the Environment. Part I. Cycling and Characterization, John Wiley & Sons, New York, 1994.
[2] M.-J. Kim, J. Nriagu, S. Haack, Arsenic species and chemistry in groundwater of southeast Michigan, Environ. Pollut. 120 (2002) 379–390.
[3] P.L. Smedley, D.G. Kinniburgh, A review of the source, behaviour and distribution of arsenic in natural waters, J. Appl. Geochem. 17 (2002) 517–568.
[4] WHO, Arsenic in drinking water. United Nations Synthesis Report on Arsenic in Drinking Water www.who.int/water_sanitation_health/Arsenic/Arsenic/UNReptoc.htm, 2001.
[5] S.D. Faust, A.J. Winka, T. Belton, Assessment of chemical and biological significant of arsenical species in the Maurice River drainage basin (N.J). Part I. Distribution in water and river and lake sediments, J. Environ. Sci. Health A22 (1987) 203–237.
[6] R.J. Bowell, Sorption of arsenic by iron oxides and oxyhydroxides in soils, Appl. Geochem. 9 (1994) 279–286.
[7] S.L. McGeehan, D.V. Naylor, Sorption and redox transformation of arsenite and arsenate in two flooded soils, Soil Sci. Soc. Am. J. 58 (1994) 337–342.
[8] A. Violante, M. Pigna, Competitive sorption of arsenate and phosphate on different clay minerals and soils, Soil Sci. Soc. Am. J. 66 (2002) 1788–1796.
[9] H.W. Chen, M.M. Frey, D. Clifford, L.S. McNeill, M. Edwards, Arsenic treatment considerations, J. Am. Water Works Assoc. 91 (1999) 74–85.
[10] L.G. Twindell, R.G. Robins, J.W. Hohn, The removal of arsenic from aqueous solution by coprecipitation with iron (III), in: R.G. Reddy, V. Ramachandran (Eds.), Arsenic Metallurgy, TMS (The Minerals, Metals & Materials Society), Warrendale, PA, 2005, pp. 3–24.
[11] A.C.Q. Ladeira, V.S.T. Ciminelli, H.A. Duarte, M.C.M. Alves, A.Y. Ramos, Mechanism of anion retention from EXAFS and density functional calculations: arsenic(V) adsorbed on gibbsite, Geochim. Cosmochim. Acta 65 (2001) 1211–1217.
[12] L. Wang, A. Chen, K. Fields, Arsenic removal from drinking water by ion exchange and activated alumina plants, EPA/600/R-00/088, 2000.
[13] J.K. Yang, Y.Y. Chang, K.S. Kim, J.H. Jung, J.K. Park, Simultaneous Treatment of both As(III) and As(V) with iron-coated sand (ICS) and manganese-coated sand (MCS), Presented in EGU General Assembly 2005, Vienna, Austria, 2005.

[14] J.K. Yang, Y.Y. Chang, S.L. Lee, H.J. Choi, S.M. Lee, Application of iron-coated sand on the treatment of toxic heavy metals, Water Sci. Technol. Water Suppl. 4 (2005) 335–341.
[15] Y.Y. Chang, K.S. Kim, J.H. Jung, J.K. Yang, S.M. Lee, Application of iron-coated sand and manganese-coated sand on the treatment of both As(III) and As(V), Water Sci. Technol. 55 (2007) 69–75.
[16] J.A. Wilkie, J.G. Hering, Rapid oxidation of geothermal arsenic(iii) in streamwaters of the Eastern Sierra Nevada, Environ. Sci. Technol. 32 (1998) 657–662.
[17] S.L. Lo, H.T. Jeng, C.H. Lai, Characteristics and adsorption properties of iron-coated sand, Water Sci. Technol. 35 (1997) 63–70.
[22] D.W. Oscarson, P.M. Huang, W.K. Liaw, Role of manganese in the oxidation of arsenite by freshwater lake sediments, Clays Clay Miner. 29 (1981) 219–225.
[18] S. Goldberg, C.T. Johnston, Mechanisms of arsenic adsorption on amorphous oxides evaluated using macroscopic measurements, vibrational spectroscopy, and surface complexation modeling, J. Colloid Interface Sci. 234 (2001) 204–216.
[19] G.A. Waychunas, B.A. Rea, C.C. Fuller, J.A. Davis, Surface chemistry of ferrihydrite. 1. EXAFS studies of the geometry of coprecipitated and adsorbed arsenate, Geochim. Cosmochim. Acta 57 (1993) 2251–2269.
[20] S. Fendorf, M.J. Eick, P. Grossl, D.L. Sparks, Arsenate and chromate retention mechanisms on goethite. 1. Surface structure, Environ. Sci. Technol. 31 (1997) 315–320.
[21] M.M. Ghosh, J.R. Yuan, Adsorption of arsenic and organoarsenicals on hydrous oxides, Environ. Prog. 6 (1987) 150–157.